PCCP

Accepted Manuscript

ROYAL SOCIETY OF CHEMISTRY

www.rsc.org/pccp

Electronically Excited States of PANH Anions

Mallory L. Theis* Alessandra Candian†

Alexander G. G. M. Tielens‡ Timothy J. Lee§

Ryan C. Fortenberry¶

May 6, 2015

Abstract

The singly deprotonated anion derivatives of nitrogenated polycyclic aromatic hydrocarbons (PANHs) are investigated for their electronically excited state properties. These include single deprotonation of the two unique arrangements of quinoline producing fourteen different isomers. This same procedure is also undertaken for single deprotonation of the three nitrogenation isomers of acridine and the three of pyrenidine. It is shown quantum chemically that the quinoline-class of PANH anion derivatives can only produce a candidate dipole-bound excited state each, a state defined as the interaction of an extra electron with the dipole moment of the corresponding neutral. However, the acridine- and pyrenidine-classes possess valence excited states as well as the possible dipole-bound excited states where the latter is only possible if the dipole moment is sufficiently large to retain the extra electron; the valence excitation is independent of the radical dipolar strength. As a result, the theoretical vertically computed electronic spectra of deprotonated PANH anion derivatives is fairly rich in the 1.5 eV to 2.5 eV range significantly opening the possibilities for these molecules to be applied to longer wavelength studies of visible and near-IR spectroscopy. Lastly, the study of these

*Georgia Southern University, Department of Chemistry, Statesboro, GA 30460 U.S.A.

†Leiden Observatory, Leiden University, PO Box 9513, 2300 RA Leiden, The Netherlands

‡Leiden Observatory, Leiden University, PO Box 9513, 2300 RA Leiden, The Netherlands

§Mail Stop 245-1 NASA Ames Research Center, Moffett Field, California 94035-1000, U.S.A.

¶Georgia Southern University, Department of Chemistry, Statesboro, GA 30460 U.S.A. E-Mail: rfortenberry@georgiasouthern.edu

systems is also enhanced by the inclusion of informed orbital arrangements in a simply constructed basis set that is shown to be more complete and efficient than standard atom-centered functions.

1 Introduction

Polycyclic aromatic hydrocarbon (PAH) molecules, are the subjects of study for a large variety of disciplines, spanning from environmental studies to molecular physics through biology and chemistry. In particular, they are one of the major thrusts of research in modern astrochemistry.[1] They are almost universally accepted as carriers of the Unidentified Infrared Bands (UIBs) or, equivalently, Aromatic Infrared Bands (AIBs), a family of interstellar emission features dominating the infrared spectrum of many diverse astronomical sources.[2] PAH molecules are also invoked in the explanation of other interstellar spectroscopic features such as the 220 nm bump in the interstellar extinction curve, the anomalous microwave emission, and the Diffuse Interstellar Bands (DIBs).[3–5] The DIBs - the 'longest standing problem in molecular astrophysics' - are some hundreds of absorption features observed across a broad spectrum stretching from the near-ultraviolet to near-IR wavelength range.[6] Neutral PAHs, as well as cations, have been proposed as possible carriers of many DIB features because their electronic transitions fall in this spectral range,[7,8] but, so far, not a single chemical carrier has been unambiguously identified within the DIBs.[9,10] More recently, PAHs are reasoned to explain the presence of large anions detected in Titan's atmosphere,[11] further cementing their relevance to the field.

The vibrational spectroscopy of PAH molecules has been studied in detail both experimentally and theoretically.[12] Because they are very regular systems, their spectra remain fairly consistent, even across isomers, with the caveat that certain features may often stand out.[13–16] Inclusion of a nitrogen atom into a PAH molecule (creating a so-called PANH) can sufficiently alter the infrared spectra, with some features being noticeably shifted.[17,18] Removal of hydrogens further alter the spectra of PAHs and PANHs creating new and different IR features.[19,20] Additionally, PAH/PANH anions

can easily form due to the distribution of the electrons over the surface, especially in the π cloud. As a result, PAH/PANH anions are also relatively stable[21,22] with different spectroscopic trends.[23,24] This has led to a recent interest in the role that PAH and PANH anions may play in the chemistry and physics of the interstellar medium (ISM).[24,25]

It is believed that many anions form in the ISM through electron capture via what is called a dipole-bound excited state.[26–28] Dipole-bound states are closely related to Rydberg states where an electron exists in a diffuse orbital such that the remaining positively-charged core of the molecule functions like a proton, and the electron exists in a hydrogen-atom-like orbital. In dipole-bound excited states of anions, removal of the electron to such a diffuse molecular perimeter would produce a neutral molecular core, but it is the dipole moment of the corresponding radical that retains the extra electron. The absolute minimum dipole moment required to perform such a retention is 1.625 D,[29] but this has been refined with modern techniques to at least 2.0 D and potentially closer to 2.5 D.[30–34] A second dipole-bound state of singly charged anion requires a dipole moment of at least 9.0 D,[35] limiting reasonable expectations of dipole-bound states to one per molecule.

If the ground state of an anion is actually valence in nature, a dipole-bound state may function as an excited state producing electronic absorption or emission features for anions.[36] This is most easily constructed for closed-shell anions and corresponding neutral radicals. Dipole-bound electronic excitation in anions is known experimentally for a few small anions,[37–40] prompting well-reasoned speculation that one of these, CH_2CN^-, could be the carrier of a DIB.[41,42] The excitation to this state takes place right at the electron binding energy (eBE) since dipole-bound states are weakly bound by definition.[36,43] However, it has recently been shown through theoretical methods that small anions may even possess valence excited states[27,44–47] corroborating a similar result for larger systems[48–50] indicating that anionic electronic spectroscopy may not be as irrelevant as previously believed. Additionally, most electronic excitations of anions, whether valence or dipole-bound, appear toward the red-end of the electromagnetic spectrum if not into the near-IR making them ideal candidates for DIB

carriers.[41,47,51]

In the present work, we are bridging many of the above themes into one body. The structures, stabilities, eBEs, and electronically excited states of closed-shell, singly-deprotonated PANH anions, like previous deprotonated PAH studies,[24,25] are explored quantum chemically in a manner building upon that utilized previously for small anions.[44–47,51] PANHs are chosen since even dehydrogenated PAHs will have small dipole moments, but presence of the nitrogen heteroatom will increase the likelihood of the aromatic system possessing a significant dipole moment.[52,53] Thus, whether valence excited states are present or not, dipole-bound excited states are possible.

2 Computational Details

Geometry optimizations of the neutral radicals and their corresponding anions of the various PANH isomers of the included quinoline, acridine, and pyrenidine molecular classes are computed using the Gaussian 09 program[54] with the B3LYP[55,56] density functional and the 6-31+G** basis set[57] previously shown to work quite well for PAHs of this size.[24] The relative anionic and radical energies, as well as the radical dipole moments, are determined from these optimized geometries. For the sake of this study, the minimum dipole moment of the neutral radical necessary for a state in a corresponding anion to be classified as dipole-bound is chosen to be 2.0 D in order to ensure that no possible dipole-bound excited states of these systems are left unexplored. Again, there is no minimum dipole moment required for a valence excited state to be present in any anion since it exists independently of the electric dipole.

Vertical excitation computations of the closed-shell anions are based on the B3LYP/6-31+G** optimized geometries of the ground $1\ ^1A'/1\ ^1A_1$ states of each isomer. They require use of spin-restricted Hartree-Fock (RHF) wave functions.[58] The excited states of the different isomers of the three classes are computed vertically through equation-of-motion coupled cluster theory at the singles and doubles level (EOM-CCSD)[59,60] within the PSI4 suite of quantum chemistry programs.[61] The cc-pVDZ, aug-cc-pVDZ, d-aug-cc-pVDZ, t-aug-cc-pVDZ basis sets[62,63] (abbreviated as pVDZ, apVDZ, dapVDZ,

and tapVDZ, respectively) showcase either a decrease or consistency in excitation energy for a given state across the diffuseness range for the selected basis sets. This provides for determination of an anion's excited state to be dipole-bound or valence, respectively, as has been demonstrated on many occasions previously.[44–47,51]

Additionally, highly diffuse *s*-type orbitals are constructed in an even-tempered fashion building upon those already employed to describe Rydberg states of smaller molecules.[64] These specific basis sets are formulated and implemented in the hopes of bypassing the need to use the very large localized or atom-centered atomic orbital basis functions usually necessary to reach an adequate degree of diffuseness in the molecular orbitals mirroring previous work on dipole-bound ground state anions.[65] Recent work[66] has analyzed the exact basis scheme utilized in the present study and has shown that four of these *s*-type functions are adequate for the description of dipole-bound excited states in small anions for the level of computational accuracy included in this study (0.01 eV). Additionally, the recent work shows that vertical excitation energies are nearly invariant with respect to the centering of these diffuse orbitals. In other words, placement of the extra diffuse orbitals at the center-of-mass, the center-of-charge, or elsewhere does not affect the vertical excitation energy within computational accuracy.[66] These orbitals are so large that the difference between the center-of-charge and the center-of-mass, or even one extreme side of the molecule versus the other side, are insignificant by comparison. Since most quantum chemistry programs reorient the molecular origin to the center-of-mass, we are choosing to center these four *s*-type orbitals at the molecular center-of-mass for simplicity and consistency.

The use of these additional diffuse functions only adds four functions to the existing basis set of choice thus minimizing computational cost. In order to determine if these four additional *s*-type functions (notated as "+4s") are adequate for the larger $PANH^-$ systems as compared to small anions, the quinoline anion derivatives are tested for their behavior with the standard set of *n*-aug-cc-pVDZ basis sets as well as the apVDZ+4s and dapVDZ+4s basis sets. The larger acridine and pyrenidine computations with the tapVDZ basis set are significant computations of more than 400 basis functions and are very expensive for EOM-CCSD. As such, the vertical excitation energy computa-

tions for the conformational isomers of the acridine anion derivatives make use of the pVDZ, apVDZ, dapVDZ, and apVDZ+4s basis sets. Computations for the isomers of pyrenidine anions only utilize the pVDZ, apVDZ, apVDZ+4s bases.

Electron binding energies for all molecules are computed using the CFOUR computational chemistry package[67] with the equation-of-motion ionization potential (EOMIP) formalism at the CCSD level of theory. The EOMIP wave function is modified to have one less creation operator than the standard EOM model providing for electron removal.[68] Since high levels of diffuseness are not present in the corresponding radical's structure, only the apVDZ basis set is required for EOMIP-CCSD computations producing the eBEs. The 1.523 eV EOMIP/apVDZ vertical eBE of CH_2CN^- is within 0.02 eV of the experimental 1.543 eV eBE indicating some level of reliability for these computations.[30,37,42,44,66]

3 Results and Discussion

3.1 Geometries and Relative Energies

The quinoline and isoquinoline species are the smallest of the PANHs studied and are labeled for simplicity as "N1" and "N2," respectively. The nitrogenation of anthracene creates three distinct isomeric species: acridine ("N1"), 1-aza-anthracene ("N2"), and 2-aza-anthracene ("N3"). Like acridine, replacement of a methyine group with a nitrogen atom in pyrene produces, again, three distinct isomers: pyrenidine, 1-aza-pyrene and 2-aza-pyrene labeled as "N1", "N2", and "N3" once more. The quinoline-class produces 14 unique isomeric derivatives with the removal of a hydrogen atom from the two nitrogenated isomers. Both the acridine and pyrenidine-classes have 23 deprotonated isomers. The nomenclature for the deprotonation is sequential based on the numbering of the adjacent carbon atom from which the proton is removed. The numbering of the carbon atoms from "1" begins at the atom adjacent to the nitrogen and continues around the molecule, as listed in Figures 1, 2, and 3. Acridine and pyrenidine, themselves, are actually C_{2v} molecules and not C_s reducing the standard number of deprotonated derivates from nine to five in each case.

Data for relative energies of both the derivative anions and radicals as well as the radical dipole moments for the quinoline-class are given in Table 1, arranged from the lowest relative energy of the anions to the highest for each class (quinoline and isoquinoline derivatives). Of the 14 possible isomers, 10 possess a dipole moment whose strength is chosen for this study to warrant exploration of a dipole-bound excited state ($>$ 2.0 D). The N1H3 isomer has the lowest relative anionic energy, but the corresponding radical has a dipole moment at 1.20 D, considerably lower than what is required to possess a dipole-bound excited state. The N1H2 radical has a large enough dipole moment (2.01 D) to retain an electron in a dipole-bound state, and its corresponding anion is the lowest energy quinoline-class anion considered. The N2H7 isomer has the lowest relative energy among the radicals, but the corresponding anion is 0.433 eV above the N1H2 anion. The radicals all fall within 0.34 eV of one another except for the N1H1 isomer which is more unstable due to the overlap between the lone pair on the nitrogen and the radical electron on the adjacent carbon.

Of the 23 unique acridine-class isomers, 16 anions are candidates to possess a dipole-bound excited state since the corresponding radicals have dipole moments of $>$ 2.0 D, as shown in Table 2. The N1H5 isomer is the lowest energy deprotonated acridine anion derivative, but the corresponding radical's dipole moment is only computed to be 1.06 D, too small for a dipole-bound excited state. The N1H2 anion isomer is 0.469 eV higher in energy and has a corresponding radical dipole moment, 2.76 D, strong enough to support a dipole-bound state. A direct pathway between the 2 anion isomers would require 3 H-shifts making it is unlikely to take place prospectively isolating each system within its potential well. The N2H3 anion is the lowest energy 1-aza-anthracene derivative, but its corresponding radical shows a dipole moment of only 1.35 D. For the N2's, it is needed to go as high as 0.320 eV in order to find an anionic isomer with a corresponding radical dipole moment greater than 2 D. The N3H8 isomer is 0.175 eV higher in energy than N1H5 and has a 3.36 D radical dipole moment, large enough to support a dipole-bound excited state. The N3H5 radical is the lowest energy neutral in the acridine-class, but the corresponding anion is 0.458 eV above the N1H5 minimum. Within each class of acridine derivatives, the highest energy isomers

are within ≈0.6 eV of lowest. The radicals exhibit two exceptionally low energies for the N3H5 and N3H6 isomers. The N2H1 isomer is the next most stable radical at 1.236 eV above N3H5, but N2H9, the least stable radical, is only 1.641 eV above the minimum. Hence, the radicals appear to fall into two subgroups, the significantly more stable N3H5 and N3H6 isomers and the rest. One could argue that N3H5 and N3H6 will represent the vast majority of the acridine PANH anions since formation through a dipole-bound state is likely to require the neutral radical, and these are far and away the two most stable neutral radical isomers.[26,27]

Twenty-three distinctive deprotonated isomers of the pyrenidine-class are possible with 17 of the corresponding neutral radicals possessing a dipole moment larger than 2.0 D; these are given in Table 3. N1H8 is the lowest energy anion, and its corresponding radical has a has a large dipole moment at 2.82 D. N2H5 is the lowest energy isomer of the 1-aza-pyrene derivatives, but its radical dipole moment cannot sustain a dipole bound state. The next most stable, and virtually isoenergetic, anion isomer is N2H2 with a 2.90 D dipole moment for the corresponding radical. N3H4 is the most stable of the 2-aza-pyrene derivatives, and it has a strong dipole moment (2.47 D). N1H9, N2H1, and N3H1 are the most stable radicals. For each class of pyrenidine derivatives, the remaining isomers are within ≈0.3 eV of the most stable. Hence, the relative energies of the isomers is much less for this set of larger PANH derivatives indicating that the isomeric energy differences may begin to level out for larger and larger PANH and PAH deprotonated derivatives.

Exploration as to possible links between the relative energies of the radicals, relative energies of the anions, and the dipole moments was undertaken as a part of this project. However, no correlation could be established between the relative energies or dipole moments and: 1) each other; 2) the position of the carbene carbon and the nitrogen in the anion; and 3) the radical carbon and the nitrogen. Hence, from the current sample set, explicit computations appear necessary to establish the relative energies and dipole moments reported in Tables 1, 2, and 3. Inclusion of more PANH anions may alter this conclusion, but the current data do not show any strong relationships as outlined.

3.2 Vertical Excitation Energies

3.2.1 Quinoline Derivatives

As seen in Table 4, all 10 isomers of the quinoline-class with a dipole moment > 2.0 D show a steady decrease in energy with an increase in diffuseness of the basis set for the $2\ ^1A'$ state. The wave function character for the transition of this state in each isomer is dominated by the a' HOMO into the a' LUMO, lending further credence to the conclusion that if these excited states exist, they are dipole-bound. Full conclusion of this hypothesis is from the apVDZ+4s and dapVDZ+4s excitation energies which are, without exception, identical to one another and are actually slightly lower in energy than the tapVDZ results. This highlights that the four additional *s*-type orbitals actually describe dipole-bound excitation better than the linear combination of atomic orbitals approach in the more traditional, even-tempered tapVDZ basis set. Additionally, the excitation energy for the most diffuse basis set (tapVDZ) is quite close to the eBE, but the apVDZ+4s and dapVDZ+4s energies are either perfectly coincident with the vertical eBEs or are higher by no more than 0.01 eV, the present expected level of computational accuracy. Hence, no further gain is attained in the description of the excitation with the utilization of basis sets larger than the apVDZ+4s including dapVDZ, tapVDZ, and dapVDZ+4s. This decreases the number of basis functions necessary to describe these quinoline-class dipole-bound excited states from 512 in tapVDZ to 288 in apVDZ+4s significantly reducing the computational cost for determining whether excited states of anions are valence, dipole-bound, or if they exist at all.

The oscillator strengths (f) for the dapVDZ and apVDZ+4s basis sets are also given in Table 4. The comparison between these two values for each isomer further supports the designation of the $2\ ^1A'$ states as dipole-bound. Since the diffuseness of the basis set increases for the apVDZ+4s values and f subsequently decreases, the oscillator strength for the less diffuse basis sets cannot be trusted. The energetic results show that the choice of basis for the present "+4s" diffuse functions is adequate for indicating that dipole-bound excited states of larger anions may exist in addition to similar claims for smaller species.[66]

Energies of the potential 1 $^1A''$ states are also given herein. These states are formed with excitations from the a' HOMO once more but this time into a higher energy a'' virtual orbital. In theory, the virtual orbital of interest is actually the $n = 6$ orbital for the π particle-in-a-box (PIB), particle-on-a-ring, particle-on-a-figure-eight, etc. simple quantum chemical model. There is little transformation of energy as the basis set becomes more diffuse beyond the apVDZ level, which would indicate the presence of a valence excited state. However, the energies of these states become higher than the corresponding eBEs and dapVDZ dipole-bound state excitation energies showing that valence states are not accessible in the quinoline-class of anions.

The UV-Vis spectra for the quinoline-class of PANH anions are all closely associated but are distinct enough for them to be distinguished. The converged, apVDZ+4s dipole-bound excitation energies range from 1.59 eV for N2H7 to 2.08 eV for N2H6. All of these vertical excitations are toward the red end of the electronic spectrum. Adiabatic computations are computationally expensive and beyond the scope of the present work, but, even so, the geometries should not change dramatically upon electronic excitation. The dipole-bound excited state geometries should, in theory, be closely related to the neutral radicals. The differences in the two geometries computed here are less than 0.01 Å for the bond lengths and 4.0° for most of the bond angles of these molecules. The largest bond angle discrepancies come at the carbene carbon and can be as much as 8.0° between the neutral-radical and the ground state anion. The anion carbene C−C−C angles (and those adjacent) are smaller than their neutral-radical counterparts due to more electron pair repulsion in the anion's double occupation of the a' orbital. As a result, the adiabatic excitation energies for these PANH anion derivatives will be slightly red-shifted since geometrical response to the change in wave function excitation is not conserved in the present vertical computations, but the vertical values presented here should correspond to experimentally measured absorption spectra.

3.2.2 Acridine Derivatives

Like the quinoline derivatives, it is shown in Table 5 that the 2 $^1A'$ states of the acridine anion derivatives are dipole-bound. These HOMO-LUMO, a' to diffuse s-type orbital

transitions showcase a clear decrease in the excitation energy when moving from the pVDZ to the apVDZ+4s bases. The dapVDZ excitation energies demonstrate a further intermediacy, but the near-perfectly coincident nature of the vertical eBEs to the apVDZ+4s excitation energies further corroborates that the 2 $^1A'$ states may exist in these larger PANH anion derivatives in these energy regimes.

However, unlike the quinoline PANH anion derivatives, the energy of the 1 $^1A''$ states are found to be lower than that of the eBE and the 2 $^1A'$ excitation energy for each isomer. In other words, *the acridine anion derivatives all possess valence excited states* since the excitation energy remains largely consistent over basis sets from apVDZ to dapVDZ to apVDZ+4s. The valence excited states are the result of a' HOMO excitations into the $n = 8$ π PIB-like valence, virtual orbitals. Both of these orbitals are visually depicted for the N1H5 isomer in Figure 4 clearly showing the isolated nature of the HOMO on the carbene carbon and the distinctly different π PIB-like "LUMO" accepting virtual orbital, LUMO in the sense of the PIB model and not the molecular system as a whole. Additionally, the f values indicate that the 1 $^1A''$ states are valence since they do not change between the apVDZ and apVDZ+4s levels, but the 2 $^1A'$ state f values decrease by orders of magnitude upon inclusion of the diffuse functions. It is interesting to note that the pVDZ energies for the 1 $^1A''$ excited state are lower than the larger basis sets.

With the possibility of valence excited state formation, it is no longer required to have a dipole moment greater than 2.0 D, 2.5 D, or any strength in order to form an excited state in one of these PANH anions. Thus, the seven isomers with lower dipole moments are also tested (Table 6) and give clear indication of possessing valence excited states even though dipole-bound states are not possible. The lowest energy excitation present in these vertical computations is the valence 1 $^1A'' \leftarrow 1$ $^1A'$ 1.47 eV transition in N2H1. The valence excitations can have excitation energies as high as 2.31 eV for N3H8. The dipole-bound excited state energies range from 1.71 eV in N2H1 to 2.49 eV for N1H5. It is interesting to note that the highest energy excitations of either type (valence or dipole-bound) typically correspond to the most stable anions, while excitation of the lowest energy correspond to the least stable anions. Additionally, the

dipole-bound vertical excitations of the acridine-class are also higher in energy than their quinoline counterparts in most cases. However, they all still fall within the same 1 eV range between 1.5 eV and 2.5 eV. The f values for the valence excited states of the acridine derivatives are also usually orders of magnitude larger than the dipole-bound states within a given isomer. N1H5, N2H3, N2H1, N2H2, and N3H5 all have oscillator strengths on the order of 2×10^{-3}. By contrast the brightest dipole-bound states are for N3H5 and N3H6 with $f = 7 \times 10^{-5}$.

3.2.3 Pyrenidine Derivatives

The data in Table 7 indicate the pyrenidine derivatives with dipole moments > 2.0 D all posses 2 $^1A'$ excited states with dipole-bound behavior for HOMO-LUMO a' to s-type transitions. Additionally, the valence excited 1 $^1A''$ states are also accessible by most in this set with excitations out of the a' HOMO into the $n = 9$ π PIB-like a'' higher energy virtual orbital. Hence, the remaining small-dipole isomer excitation energies and eBEs are given in Table 8. The orbitals involved in a valence excitation are shown in Figure 5 for the N1H8 isomer. Once more, the a' HOMO is largely isolated to the lone pair on the carbene carbon with the virtual valence orbital of the π PIB-like system. The valence excited states, again, have lower energies than the dipole-bound excited states within given isomers, and the apVDZ+4s dipole-bound excitation energies are coincident with the vertical eBEs that could be produced. The EOMIP wave function becomes unstable for many of the desired isomers. As a result, the apVDZ+4s dipole-bound excited state energies are understood here also to represent the eBEs, and this trend is observed in the quinoline and acridine-classes corroborating such a conclusion. The apVDZ+4s excitation energy-interpreted eBEs are marked in Tables 7 and 8 with asterisks (*).

Since the acridine anion derivatives are larger than the quinoline anion derivatives, it is understandable that the valence excitation energy is lowered from a PIB perspective. This should progress to the even larger pyrenidine anion derivatives, as well. However, the N3H4, N3H2, and N3H3 anion isomers actually have valence excited states higher in energy than the dipole-bound excited states and above the vertical eBEs

where the latter are computed explicitly (N3H3). The N3H1 isomer appears to possess a valence excited state, but this excitation energy is within 0.01 eV of the dipole-bound state. The N3H5 isomer has a larger (0.16 eV) splitting between the two excited states with the valence state lower, but the dipole moment of the corresponding neutral radical is too small to support a dipole-bound state. Since this isomer is actually C_{2v}, symmetry dictates the hard zero oscillator strength. The reason for the aversion to valence excited states for the "N3" (2-aza-pyrene) isomers comes from the excitations themselves. They are once more out of the a'/a_1 HOMO but into the $n = 10$ π PIB-like orbital and not the $n = 9$. Hence, the orbitals or the higher pseudo-symmetry of the anion (or both) disfavors the PIB LUMO for the PIB LUMO+1, and the formation of valence excited states is not preferred over the dipole-bound excitations in the "N3" pyrenidine anion derivatives. Additionally, the N1H1 valence excited state is 0.01 eV higher than the dipole-bound state at 2.05 eV. However, the excitation for the valence excited state is of the standard type (a' HOMO into the $n = 9$ π PIB-like valence virtual orbital) indicating that the valence excited state may yet be possible in this anion.

Fascinatingly, the vertical excitation energies for the pyrenidine-class of anion derivatives still fall within the 1.5 to 2.5 eV range, the same for the smaller quinoline and acridine-classes. The f values are also of similar magnitude. As a result, the electronic excitation peaks of deprotonated PANH anion derivatives, whether valence or potentially dipole-bound, all cluster at the red end of the visible portion of the spectrum.

4 Astrophysical Implications

The relevance of PAH anions in astrophysical environments has been modeled by several authors.[69–71] This previous work has shown that the presence of these species is primarily influenced by the balance between the strength of the radiation field and the electron density, even though molecular size also plays a role. Models predict PAH anions readily form through radiative electron attachment in dense clouds; they can even become the dominant anionic species if the local abundance of PAH molecules is high.[72] Modeling has also shown that PAH anions can deeply affect the chemistry of

the cloud, increasing the abundance of small C-bearing molecules.[71]

However, in the above models, only PAH radical anions are considered, which can easily be neutralized due to their low eBEs. Differently, closed-shell PAH anions as well as the PANH anions studied here exhibit higher eBEs[24,25] possibly increasing their abundance relative to radical PAH/PANH anions in dense clouds.[73] Interestingly enough, the anions so far detected in the interstellar medium are all carbon-bearing, deprotonated molecules: C_4H^-, C_6H^-, C_8H^-, CN^-, C_3N^-, and C_5N^-.[74–81] Most of these molecules are proposed to form through radiative attachment of an electron to a neutral species (X) producing an electronically excited anion (X^{-*}). The electronically excited anion will then relax to its ground state.[26,27,82–85] Dipole-bound states can act as the required excited states in this process, and are likely to be such due to their large reaction cross-sections. Most of the PANH anions examined in this study possess dipole-bound states, making radiative attachment an attractive mechanism for their interstellar formation.

Since nitrogen is one of the most abundant elements in space, the possibility of N-substituted PAHs in space has been extensively studied, especially in relation to the AIBs.[53,86–88] Experimental studies[89,90] show that small N-heterocycles are quite susceptible to UV irradiation, but in the low irradiated environment of a dense cloud, they would be able to survive the average lifetime of the cloud.[89] All of these individual pieces of evidence further support the closed-shell nitrogen-substituted PAH molecules studied here as strong candidates for additions to the inferred PAH anion populations present in dense clouds. Additionally, the dehydrogenated PANH neutral radicals possess large electric dipole moments, mostly due to the presence of the nitrogen atoms. In principle, this could allow detection of these species through microwave spectroscopy in cold clouds,[52,91] but the detection can be compromised by small rotational constants, high partition functions, and unknown size/population distribution.

Finally, from a spectroscopic point of view, the existence of valence excited states, especially, for the deprotonated PANH anion derivatives in the 1.5-2.5 eV (or 495-826 nm) range for vertical computations makes these molecules fascinating candidates as carriers of the DIBs. In particular, given the low oscillator strength of these states and

the inferred total abundance of PAH in the ISM, PANH anion derivatives possibly could be responsible for the less strong DIBs. In this regard, it is interesting to note that the same PAH structure can give rise to different isomers and, hence, to different, unique spectra helping to account for the large number of absorption peaks without exceeding the measured carbon budget.

5 Conclusions

In all, several take-home messages are provided by this work. First, the "+4s" functions are better alternatives to linear combination approaches for the modeling of highly-diffuse orbitals for dipole-bound excited states of anions. They save tremendous amounts of computational time making EOM-CCSD computations of PANHs possible and actually perform better than the t-aug-cc-pVDZ basis set corroborating similar results for small anions.[66] Second, as the size of the PANHs increase, the relative isomeric energy range for the different deprotonated or dehydrogenated forms contracts with the exception of the extreme radical outliers: N1H1 quinoline and N3H5/N3H6 acridine. This makes them likely to be produced together in some astronomical objects but not likely to be created spontaneously in the temperatures of the ISM. Interstellar detection of these systems would, consequently, provide some astrophysical insights into the region of their potential creation.

Third, the smaller PANH anions (the quinoline-class) do not support valence excited states, but the larger PANH anions (the acridine and pyrenidine-classes) do. This paves the road to search for dipole-bound and valance excited states on even larger PA(N)H anions. Interestingly, the 2-aza-pyrene ("N3" pyrenidine derivative) anion derivatives do not possess valence excited states since these excitations prefer to access the PIB π system's LUMO+1 orbital instead of the PIB LUMO. Fourth, the range of the excitations, regardless of the anion, all fall within the 1.5 to 2.5 eV excitation energy range, which is remarkable for molecules of such different sizes. Fifth, the valence excitation oscillator strengths are fairly small but still detectable for the possible abundances of these types of systems. Sixth and finally, these candidate dipole-bound

excited states will certainly enhance the possibility for the formation of the anions in the first place, and the presence of the brighter valence excited states are promising candidates for future analysis as carriers of DIBs or other unresolved spectra falling in or just shy of the near-IR region of the electromagnetic spectrum.

6 Acknowledgements

Start-up funds provided by Georgia Southern University (GSU) as well as a GSU College of Science and Mathematics "Interdisciplinary Pilot Grant" supported the work undertaken by MLT and RCF. Studies of interstellar PAHs at Leiden Observatory are supported through advanced European Research Council Grant 246976. This material is based upon work supported by the National Aeronautics and Space Administration through the NASA Astrobiology Institute under Cooperative Agreement Notice NNH13ZDA017C issued through the Science Mission Directorate. Figures 1, 2, and 3 are produced with the CheMVP program developed at the Center for Computational Quantum Chemistry at the University of Georgia, and the authors are thankful to the developers for the use of this program. Figures 4 and 5 are generated with the WebMO[92] computational chemistry graphical user interface. Part of the calculations were performed at the SARA supercomputer center in Amsterdam, Netherlands (project MP-270-13). We are also grateful for access to the University of Nottingham High Performance Computing Facility. MLT and RCF would also like to acknowledge Prof. Clayton Heller of the GSU Department of Physics and Astronomy for the use of his computer system necessary to complete many of the initial large excited state computations.

References

[1] A. G. G. M. Tielens, *Rev. Mod. Phys.*, 2013, **85**, 1021–1081.

[2] E. Peeters, EAS Publications Series, 2011, pp. 13–27.

[3] G. Mulas, G.and Malloci, C. Joblin and C. Cecchi-Pestellini, EAS Publications Series, 2011, pp. 327–340.

[4] N. Ysard, M. Juvela and L. Verstraete, *Astron. Astrophys.*, 2011, **535**, A89.

[5] A. Tielens, *The Physics and Chemistry of the Interstellar Medium*, Cambridge University Press, Cambridge, UK, 2005.

[6] P. J. Sarre, *J. Mol. Spectrosc.*, 2006, **238**, 1–10.

[7] F. Salama, G. A. Galazutdinov, J. Krelowski, L. J. Allamandola and F. A. Musaev, *Astrophys. J.*, 1999, **526**, 265–273.

[8] F. Salama, G. A. Galazutdinov, J. Krełowski, L. Biennier, Y. Beletsky and I.-O. Song, *Astrophys. J.*, 2011, **728**, 154.

[9] J. P. Maier, G. A. H. Walker, D. A. Bohlender, F. J. Mazzotti, R. Raghunandan, J. Fulara, I. Garkusha and A. Nagy, *Astrophys. J.*, 2011, **726**, 41.

[10] T. Oka and B. J. McCall, *Science*, 2011, **331**, 293–294.

[11] M. López-Puertas, B. M. Dinelli, A. Adriani, B. Funke, M. García-Comas, M. L. Moriconi, E. D'Aversa, C. Boersma and L. J. Allamandola, *Astrophys. J.*, 2013, **770**, 132.

[12] A. G. G. M. Tielens, *Annu. Rev. Astron. Astrophys.*, 2008, **46**, 289–337.

[13] D. M. Hudgins and L. J. Allamandola, *Astrophys. J. Lett.*, 1999, **516**, L41–L44.

[14] C. W. Bauschlicher, Jr., E. Peeters and L. J. Allamandola, *Astrophys. J.*, 2008, **678**, 316–327.

[15] A. M. Ricks, G. E. Douberly and M. A. Duncan, *Astrophys. J.*, 2009, **702**, 301.

[16] A. Candian, P. J. Sarre and A. G. G. M. Tielens, *Astrophys. J. Lett.*, 2014, **791**, L10.

[17] A. L. Mattioda, L. Rutter, J. Parkhill, M. Head-Gordon, T. J. Lee and L. J. Allamandola, *Astrophys. J.*, 2008, **680**, 1243–1255.

[18] H. Alvaro Galué, O. Pirali and J. Oomens, *Astron. Astrophys.*, 2010, **517**, A15.

[19] C. W. Bauschlicher and A. Ricca, *Astrophys. J.*, 2013, **776**, 102.

[20] C. J. Mackie, E. Peeters, C. W. Bauschlicher, Jr. and J. Cami, *Astrophys. J.*, 2015, **799**, 131.

[21] S. Denifl, S. Ptasińska, B. Sonnweber, P. Scheier, D. Liu, F. Hagelberg, J. Mack, L. T. Scott and T. D. Märk, *J. Chem. Phys.*, 2005, **123**, 104308.

[22] N. L. Asfandiarov, S. A. Pshenichnyuk, A. S. Vorobév, E. P. Nafikova, Y. N. Elkin, D. N. Pelageev, E. A. Koltsova and A. Modelli, *Rapid Commun. Mass Spectrom.*, 2014, 1580–1590.

[23] S. R. Langhoff, *J. Phys. Chem.*, 1996, **100**, 2819–2841.

[24] M. Hammonds, A. Pathak, A. Candian and P. Sarre, in *PAHs and the Universe: A Symposium to Celebrate the 25th Anniversary of the PAH Hypothesis*, ed. C. Joblin and A. G. G. M. Tielens, EAS Publication Series, Cambridge, UK, 2011.

[25] J. Gao, G. Berden and J. Oomens, *Astrophys. J.*, 2014, **787**, 170.

[26] M. Agúndez, J. Cernicharo, M. Guélin, M. Gerin, M. C. McCarthy and P. Thaddeus, *Astron. Astrophys.*, 2008, **478**, L19–L22.

[27] R. C. Fortenberry, X. Huang, T. D. Crawford and T. J. Lee, *Astrophys. J.*, 2013, **772**, 39.

[28] R. W. F. Carelli, F. A. Gianturco and M. Satta, *J. Chem. Phys.*, 2014, **141**, 054302.

[29] E. Fermi and E. Teller, *Phys. Rev.*, 1947, **72**, 399–408.

[30] G. Gutsev and A. Adamowicz, *Chem. Phys. Lett.*, 1995, **246**, 245–250.

[31] G. Gutsev and A. Adamowicz, *Chem. Phys. Lett.*, 1995, **235**, 377–381.

[32] M. Gutowski, P. Skurski, A. I. Boldyrev, J. Simons and K. D. Jordan, *Phys. Rev.*, 1996, **54**, 1906.

[33] F. Wang and K. D. Jordan, *J. Chem. Phys.*, 2002, **116**, 6973.

[34] K. D. Jordan and F. Wang, *Ann. Rev. Phys. Chem.*, 2003, **54**, 367–396.

[35] C. A. Coulson and M. Walmsley, *Proc. Phys. Soc.*, 1967, **91**, 31–32.

[36] J. Simons, *J. Phys. Chem. A.*, 2008, **112**, 6401–6511.

[37] K. R. Lykke, D. M. Neumark, T. Andersen, V. J. Trapa and W. C. Lineberger, *J. Chem. Phys.*, 1987, **87**, 6842–6853.

[38] A. S. Mullin, K. K. Murray, C. P. Schulz, D. M. Szaflarski and W. C. Lineberger, *Chem. Phys.*, 1992, **166**, 207–213.

[39] A. S. Mullin, K. K. Murray, C. P. Schulz and W. C. Lineberger, *J. Phys. Chem.*, 1993, **97**, 10281–10286.

[40] M. Grutter, M. Wyss and J. P. Maier, *J. Chem. Phys.*, 1999, **110**, 1492–1496.

[41] P. J. Sarre, *Mon. Not. R. Astron. Soc.*, 2000, **313**, L14–L16.

[42] M. A. Cordiner and P. J. Sarre, *Astron. Astrophys.*, 2007, **472**, 537–545.

[43] J. Simons, *Annu. Rev. Phys. Chem.*, 2011, **62**, 107–128.

[44] R. C. Fortenberry and T. D. Crawford, *J. Chem. Phys.*, 2011, **134**, 154304.

[45] R. C. Fortenberry and T. D. Crawford, *J. Phys. Chem. A*, 2011, **115**, 8119–8124.

[46] R. C. Fortenberry, *Mol. Phys.*, 2013, **111**, 3265–3275.

[47] R. C. Fortenberry, W. J. Morgan and J. D. Enyard, *J. Phys. Chem. A*, 2014, **118**, 10763–10769.

[48] T. M. Halasinski, J. L. Weisman, R. Ruiterkamp, T. J. Lee, F. Salama and M. Head-Gordon, *J. Phys. Chem. A*, 2003, **107**, 3660–3669.

[49] S. Hirata, M. Head-Gordon, J. Szczepanski and M. Vala, *J. Phys. Chem. A*, 2003, **107**, 4940–4951.

[50] C. W. Bauschlicher, *Chem. Phys. Lett.*, 2005, **409**, 235–239.

[51] R. C. Fortenberry, in *IAU Symposium 297: The Diffuse Interstellar Bands*, ed. J. Cami and N. L. J. Cox, Campbridge University Press, Cambridge, England, 2014.

[52] D. McNaughton, P. D. Godfrey, R. D. Brown, S. Thorwirth and J. Grabow, *Astrophys. J.*, 2008, **678**, 309–315.

[53] D. M. Hudgins, C. W. Bauschlicher, Jr. and L. J. Allamandola, *Astrophys. J.*, 2005, **632**, 316–332.

[54] M. J. Frisch, G. W. Trucks, H. B. Schlegel, G. E. Scuseria, M. A. Robb, J. R. Cheeseman, G. Scalmani, V. Barone, B. Mennucci, G. A. Petersson, H. Nakatsuji, M. Caricato, X. Li, H. P. Hratchian, A. F. Izmaylov, J. Bloino, G. Zheng, J. L. Sonnenberg, M. Hada, M. Ehara, K. Toyota, R. Fukuda, J. Hasegawa, M. Ishida, T. Nakajima, Y. Honda, O. Kitao, H. Nakai, T. Vreven, J. A. Montgomery, Jr., J. E. Peralta, F. Ogliaro, M. Bearpark, J. J. Heyd, E. Brothers, K. N. Kudin, V. N. Staroverov, R. Kobayashi, J. Normand, K. Raghavachari, A. Rendell, J. C. Burant, S. S. Iyengar, J. Tomasi, M. Cossi, N. Rega, J. M. Millam, M. Klene, J. E. Knox, J. B. Cross, V. Bakken, C. Adamo, J. Jaramillo, R. Gomperts, R. E. Stratmann, O. Yazyev, A. J. Austin, R. Cammi, C. Pomelli, J. W. Ochterski, R. L. Martin, K. Morokuma, V. G. Zakrzewski, G. A. Voth, P. Salvador, J. J. Dannenberg, S. Dapprich, A. D. Daniels, O. Farkas, J. B. Foresman, J. V. Ortiz, J. Cioslowski and D. J. Fox, *Gaussian 09 Revision D.01*, Gaussian Inc. Wallingford CT 2009.

[55] A. D. Becke, *J. Chem. Phys.*, 1993, **98**, 5648–5652.

[56] P. J. Stephens, F. J. Devlin, C. F. Chabalowski and M. J. Frisch, *J. Phys. Chem.*, 1994, **98**, 11623–11627.

[57] W. J. Hehre, R. Ditchfeld and J. A. Pople, *J. Chem. Phys.*, 1972, **56**, 2257.

[58] A. C. Scheiner, G. E. Scuseria, J. E. Rice, T. J. Lee and H. F. Schaefer III, *J. Chem. Phys.*, 1987, **87**, 5361–5373.

[59] J. F. Stanton and R. J. Bartlett, *J. Chem. Phys.*, 1993, **98**, 7029–7039.

[60] A. I. Krylov, *Ann. Rev. Phys. Chem.*, 2007, **59**, 433–463.

[61] J. M. Turney, A. C. Simmonett, R. M. Parrish, E. G. Hohenstein, F. A. Evangelista, J. T. Fermann, B. J. Mintz, L. A. Burns, J. J. Wilke, M. L. Abrams, N. J. Russ, M. L. Leininger, C. L. Janssen, E. T. Seidl, W. D. Allen, H. F. Schaefer III, R. A. King, E. F. Valeev, C. D. Sherrill and T. D. Crawford, *Wiley Interdisciplinary Reviews: Computational Molecular Science*, 2012, **2**, 556–565.

[62] T. H. Dunning, *J. Chem. Phys.*, 1989, **90**, 1007–1023.

[63] R. A. Kendall, T. H. Dunning and R. J. Harrison, *J. Chem. Phys.*, 1992, **96**, 6796–6806.

[64] T. J. Mach, R. A. King and T. D. Crawford, *J. Phys. Chem. A.*, 2010, **114**, 8852–8857.

[65] P. Skurski, M. Gutowski and J. Simons, *Int. J. Quant. Chem.*, 2000, **80**, 1024–1038.

[66] W. J. Morgan and R. C. Fortenberry, *Theor. Chem. Acc.*, 2015, **submitted**, year.

[67] CFOUR, a quantum chemical program package written by J.F. Stanton, J. Gauss, M.E. Harding, P.G. Szalay with contributions from A.A. Auer, R.J. Bartlett, U. Benedikt, C. Berger, D.E. Bernholdt, Y.J. Bomble, O. Christiansen, M. Heckert, O. Heun, C. Huber, T.-C. Jagau, D. Jonsson, J. JusÃl'lius, K. Klein, W.J. Lauderdale, D.A. Matthews, T. Metzroth, D.P. O'Neill, D.R. Price, E. Prochnow, K. Ruud, F. Schiffmann, S. Stopkowicz, A. Tajti, J. Vázquez, F. Wang, J.D. Watts and the integral packages MOLECULE (J. Almlöf and P.R. Taylor), PROPS (P.R. Taylor), ABACUS (T. Helgaker, H.J. Aa. Jensen, P. Jørgensen, and J. Olsen), and ECP routines by A. V. Mitin and C. van Wüllen. For the current version, see `http://www.cfour.de`.

[68] J. F. Stanton and J. Gauss, *J. Chem. Phys.*, 1994, **101**, 8938–8944.

[69] E. Dartois and L. D'Hendecourt, *Astron. Astrophys.*, 1997, **323**, 534–540.

[70] V. Le Page, T. P. Snow, and V. M. Bierbaum, *Astrophys. J. Suppl. Ser.*, 2001, **132**, 233.

[71] V. Wakelam and E. Herbst, *Astrophys. J.*, 2008, **680**, 371–383.

[72] S. Lepp and A. Dalgarno, *Astrophys. J.*, 1988, **324**, 553–556.

[73] N. J. Demarais, Z. Yang, O. Martinez, N. Wehres, T. P. Snow and V. M. Bierbaum, *Astrophys. J.*, 2012, **746**, 32.

[74] M. C. McCarthy, C. A. Gottlieb, H. Gupta and P. Thaddeus, *Astrophys. J.*, 2006, **652**, L141–L144.

[75] J. Cernicharo, M. Guèlin, M. Agùndez, K. Kawaguchi, M. McCarthy and P. Thaddeus, *Astron. Astrophys.*, 2007, **467**, L37–L40.

[76] A. J. Remijan, J. M. Hollis, F. J. Lovas, M. A. Cordiner, T. J. Millar, A. J. Markwick-Kemper and P. R. Jewell, *Astrophys. J.*, 2007, **664**, L47–L50.

[77] S. Brünken, H. Gupta, C. A. Gottlieb, M. C. McCarthy and P. Thaddeus, *Astrophys. J.*, 2007, **664**, L43–L46.

[78] P. Thaddeus, C. A. Gottlieb, H. Gupta, S. Brünken, M. C. McCarthy, M. Agùndez, M. Guèlin and J. Cernicharo, *Astrophys. J.*, 2008, **677**, 1132–1139.

[79] J. Cernicharo, M. Guèlin, M. Agundez, M. C. McCarthy and P. Thaddeus, *Astrophys. J.*, 2008, **688**, L83–L86.

[80] M. Agùndez, J. Cernicharo, M. Guèlin, C. Kahane, E. Roueff, J. Klos, F. J. Aoiz, F. Lique, N. Marcelino, J. R. Goicoechea, M. Gonzàlez Garcia, C. A. Gottlieb, M. C. McCarthy and P. Thaddeus, *Astron. Astrophys.*, 2010, **517**, L2.

[81] M. A. Cordiner, S. B. Charnley, J. V. Buckle, C. Walsh and T. J. Millar, *Astrophys. J. Lett.*, 2011, **730**, L18.

[82] T. Pino, M. Tulej, F. Güthe, M. Pachkov and J. P. Maier, *J. Chem. Phys.*, 2002, **116**, 6126–6131.

[83] M. Larsson, W. D. Geppert and G. Nyman, *Rep. Prog. Phys.*, 2012, **75**, 066901.

[84] F. Carelli, T. Grassi, F. Sebastianelli and F. A. Giantuco, *Mon. Not. Roy. Astron. Soc.*, 2013, **428**, 1181–1184.

[85] M. Satta, F. A. Gianturco, F. Carelli and R. Wester, *Astrophys. J.*, 105, **799**, 228.

[86] A. Mattioda, D. Hudgins, C. Bauschlicher, Jr., M. Rosi and L. Allamandola, *J. Phys. Chem. A*, 2003, **107**, 1486–1498.

[87] E. Peeters, S. Hony, C. Van Kerckhoven, A. G. G. M. Tielens, L. J. Allamandola, D. M. Hudgins and C. W. Bauschlicher, *Astron. Astrophys.*, 2002, **390**, 1089–1113.

[88] A. Ricca, C. W. Bauschlicher and M. Rosi, *Chem. Phys. Lett.*, 2001, **347**, 473–480.

[89] Z. Peeters, O. Botta, S. B. Charnley, Z. Kisiel, Y.-J. Kuan and P. Ehrenfreund, *Astron. Astrophys.*, 2005, **433**, 583–590.

[90] J. Bouwman, B. Sztáray, J. Oomens, P. Hemberger and A. Bodi, *J. Phys. Chem. A*, 2015, **119**, 1127–1136.

[91] Y. Ali-Haïmoud, L. M. Pérez, R. J. Maddalena and D. A. Roshi, *Mon. Not. Roy. Astron. Soc.*, 2015, **447**, 315–324.

[92] J. R. Schmidt and W. F. Polik, *WebMO Enterprise*, version 13.0; WebMO LLC: Holland, MI, USA, 2013; *http://www.webmo.net*.

Table 1: Relative anionic and radical energies (in eV) and neutral radical dipole moments (D) for the quinoline and isoquinoline derivatives.

Molecule	Relative Anionic Energy	Relative Radical Energy	Dipole Moment
N1H3	0.000	0.213	1.20
N1H2	0.133	0.272	2.01
N1H4	0.179	0.235	1.24
N1H5	0.302	0.262	1.78
N1H6	0.348	0.249	2.76
N1H1	0.473	0.669	3.02
N1H7	0.477	0.339	3.08
N2H6	0.151	0.322	2.99
N2H3	0.171	0.324	2.33
N2H2	0.176	0.316	2.76
N2H4	0.218	0.304	1.73
N2H5	0.251	0.315	2.25
N2H7	0.433	0.000	3.19
N2H1	0.619	0.123	3.47

Figure 1: “N1” Quinoline (a) and “N2” isoquinoline (b) with the carbons numbered for deprotonation or dehydrogenation.

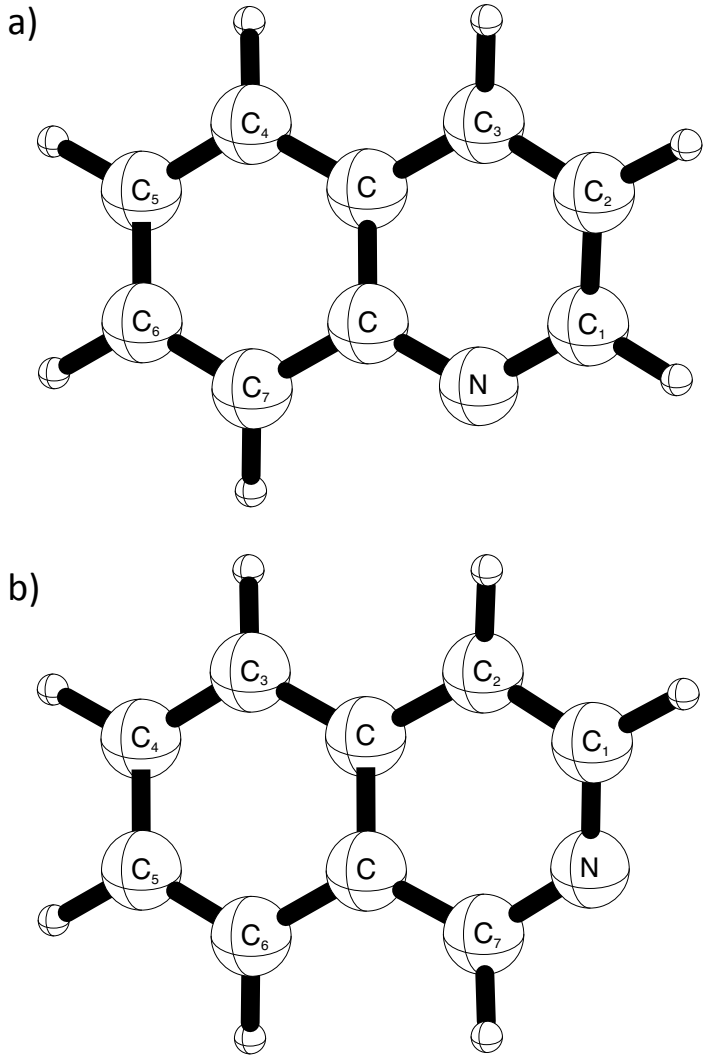

Figure 2: "N1" Acridine (a), and "N2" 1-aza-anthracene (b), and "N3" 2-aza-anthracene (c) with the carbons numbered for deprotonation or dehydrogenation.

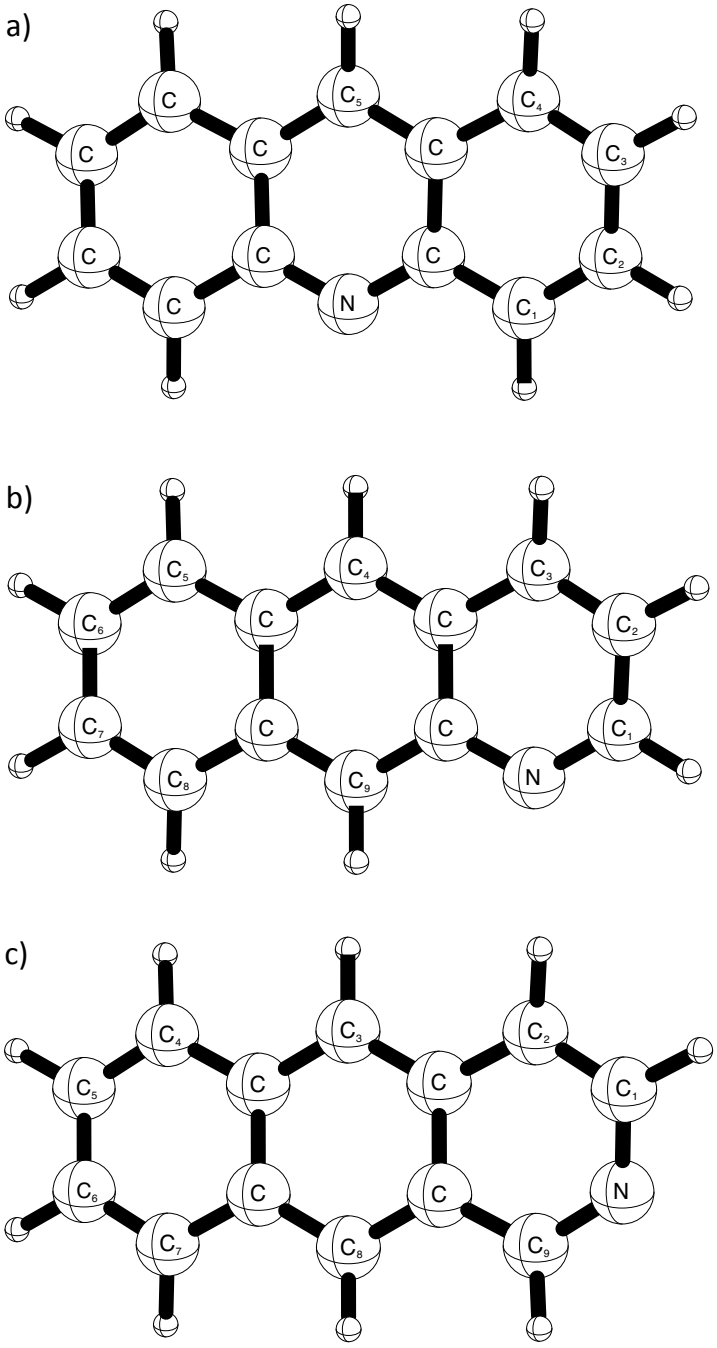

Figure 3: “N1” Pyrenidine (a), and “N2” 1-aza-pyrene (b), and “N3” 2-aza-pyrene (c) with the carbons numbered for deprotonation or dehydrogenation.

a)

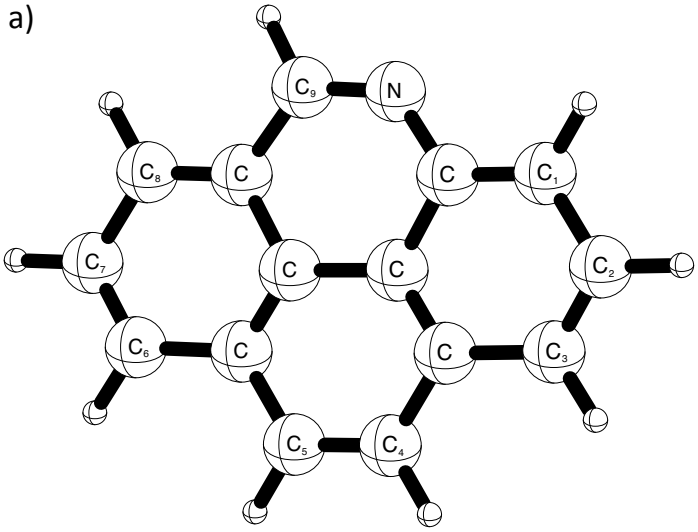

b)

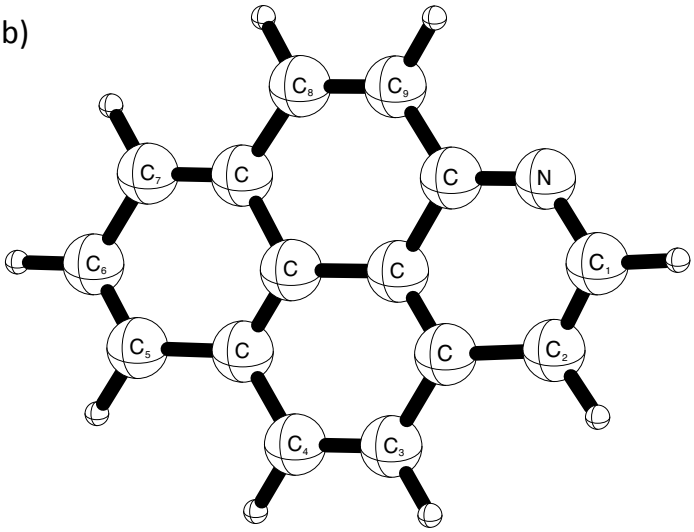

c)

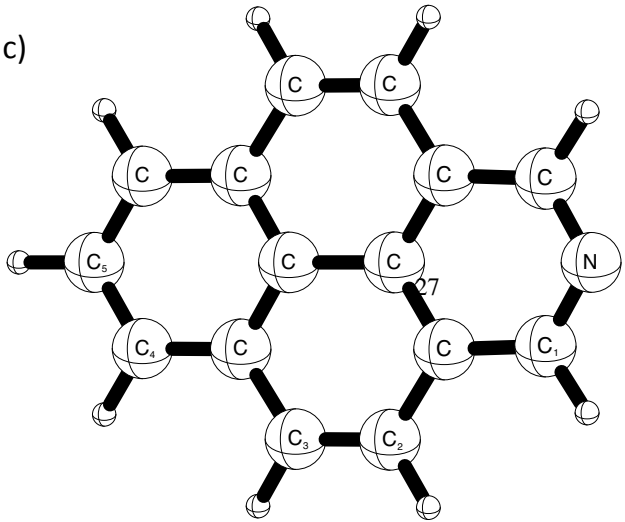

Figure 4: The acridine N1H5 anion a' HOMO (a) and the a'' $n = 8$ PIB π LUMO valence virtual orbital (b).

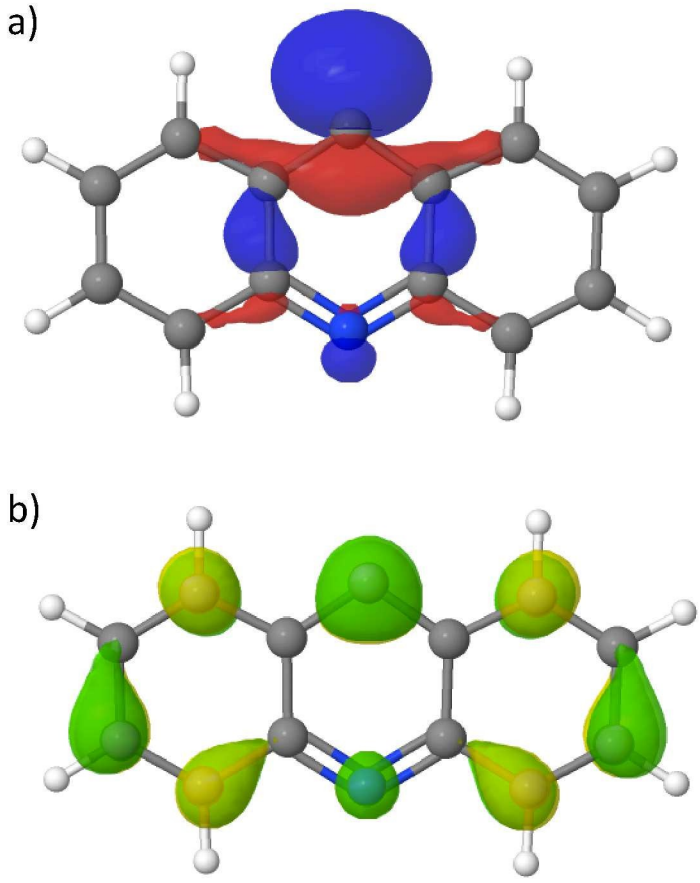

Figure 5: The pyrenidine N1H8 anion a' HOMO (a) and the a'' $n = 9$ PIB π LUMO valence virtual orbital (b).

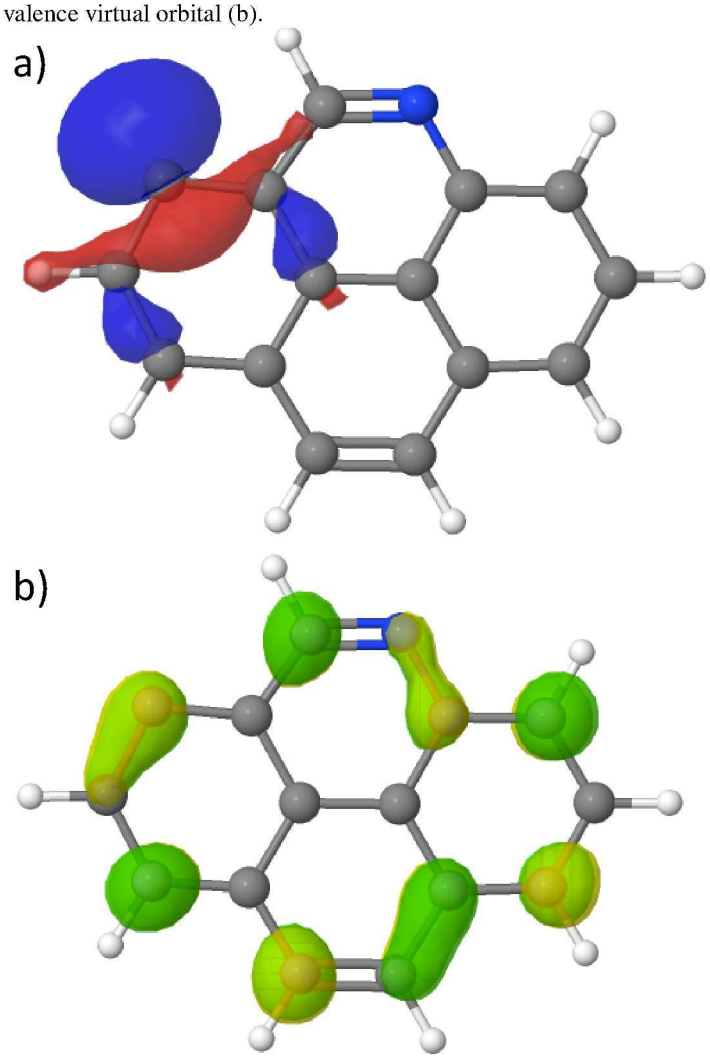

Table 2: Relative anionic and radical energies (in eV) and neutral radical dipole moments (D) for the acridine derivatives.

Molecule	Relative Anionic Energy	Relative Radical Energy	Dipole Moment
N1H5	0.000	1.450	1.06
N1H4	0.302	1.465	1.21
N1H3	0.429	1.496	1.77
N1H2	0.469	1.475	2.76
N1H1	0.616	1.570	2.91
N2H3	0.183	1.505	1.35
N2H4	0.229	1.536	1.32
N2H2	0.320	1.569	2.12
N2H5	0.445	1.548	1.31
N2H8	0.511	1.559	2.96
N2H9	0.521	1.641	2.99
N2H6	0.524	1.551	1.68
N2H7	0.537	1.550	2.73
N2H1	0.649	1.236	3.18
N3H8	0.175	1.620	3.36
N3H3	0.243	1.624	2.92
N3H7	0.385	1.608	3.09
N3H2	0.394	1.609	3.29
N3H4	0.403	1.609	2.56
N3H5	0.458	0.000	2.00
N3H6	0.470	0.015	2.46
N3H9	0.602	1.274	3.50
N3H1	0.833	1.440	3.91

Table 3: Relative anionic and radical energies (in eV) and neutral radical dipole moments (D) for the pyrenidine derivatives.

Molecule	Relative Anionic Energy	Relative Radical Energy	Dipole Moment
N1H8	0.000	0.383	2.82
N1H6	0.018	0.364	1.50
N1H3	0.147	0.375	2.31
N1H5	0.150	0.356	1.49
N1H7	0.157	0.356	2.06
N1H4	0.167	0.348	1.90
N1H2	0.319	0.349	3.20
N1H9	0.320	0.000	3.16
N1H1	0.373	0.449	3.37
N2H5	0.015	0.350	1.84
N2H2	0.019	0.367	2.90
N2H4	0.041	0.326	1.94
N2H7	0.042	0.352	2.92
N2H3	0.069	0.349	2.48
N2H6	0.159	0.339	2.06
N2H8	0.190	0.325	3.29
N2H9	0.405	0.417	3.69
N2H1	0.498	0.085	3.83
N3H4	0.109	0.432	2.47
N3H2	0.162	0.423	3.38
N3H3	0.181	0.408	2.82
N3H5	0.216	0.406	1.78
N3H1	0.384	0.161	3.54

Table 4: Vertical excitation energies (in eV), eBEs (in eV), and oscillator strengths (f) for the quinoline and isoquinoline derivative anions.

Molecule	State	pVDZ	apVDZ	dapVDZ	tapVDZ	apVDZ+4s	dapVDZ+4s	dapVDZ f	apVDZ+4s f	eBE
N1H2	$2\,^1A'$	5.65	2.94	2.26	2.06	2.03	2.03	6×10^{-2}	3×10^{-5}	2.03
	$1\,^1A''$	2.26	2.31	2.30	–	–	–	–	–	
N1H6	$2\,^1A'$	5.39	2.66	2.04	1.84	1.82	1.82	6×10^{-3}	3×10^{-5}	1.82
	$1\,^1A''$	2.20	2.25	2.23	–	–	–	–	–	
N1H1	$2\,^1A'$	5.04	2.14	1.64	1.54	1.52	1.52	7×10^{-3}	3×10^{-5}	1.52
	$1\,^1A''$	2.88	1.91	1.90	–	–	–	–	–	
N1H7	$2\,^1A'$	5.19	2.50	1.91	1.74	1.72	1.72	2×10^{-2}	9×10^{-6}	1.71
	$1\,^1A''$	2.29	2.28	2.18	–	–	–	–	–	
N2H6	$2\,^1A'$	4.31	2.65	2.18	2.09	2.08	2.08	4×10^{-2}	2×10^{-5}	2.08
	$1\,^1A''$	2.66	2.67	2.67	–	–	–	–	–	
N2H3	$2\,^1A'$	5.56	2.62	2.25	2.05	2.04	2.04	5×10^{-2}	2×10^{-5}	2.03
	$1\,^1A''$	3.06	2.62	2.48	–	–	–	–	–	
N2H2	$2\,^1A'$	4.28	2.66	2.13	2.02	1.99	1.99	5×10^{-2}	9×10^{-6}	1.98
	$1\,^1A''$	2.56	2.60	2.59	–	–	–	–	–	
N2H5	$2\,^1A'$	5.58	2.56	2.18	1.98	1.96	1.96	6×10^{-2}	4×10^{-5}	1.96
	$1\,^1A''$	2.23	2.30	2.30	–	–	–	–	–	
N2H7	$2\,^1A'$	5.19	2.24	1.72	1.62	1.59	1.59	2×10^{-1}	8×10^{-6}	1.59
	$1\,^1A''$	2.61	2.22	2.04	–	–	–	–	–	
N2H1	$2\,^1A'$	5.22	2.25	1.74	1.64	1.61	1.61	2×10^{-3}	1×10^{-5}	1.61
	$1\,^1A''$	1.97	2.05	2.02	–	–	–	–	–	

Table 5: Vertical excitation energies (in eV), eBEs (in eV), and oscillator strengths (f) for the acridine derivative anions with dipole moments $>$ 2.0 D.

Molecule	State	pVDZ	apVDZ	dapVDZ	apVDZ+4s	apVDZ f	apVDZ+4s f	eBE
N1H2	$2\,^1A'$	5.59	2.60	2.13	2.05	2×10^{-2}	4×10^{-5}	2.04
	$1\,^1A''$	1.62	1.72	1.72	1.72	1×10^{-3}	1×10^{-3}	
N1H1	$2\,^1A'$	5.35	2.46	1.99	1.91	5×10^{-3}	1×10^{-5}	1.90
	$1\,^1A''$	1.58	1.65	1.65	1.65	7×10^{-4}	8×10^{-4}	
N2H2	$2\,^1A'$	5.82	2.84	2.34	2.24	2×10^{-2}	4×10^{-5}	2.24
	$1\,^1A''$	1.79	1.89	1.89	1.89	2×10^{-3}	2×10^{-3}	
N2H8	$2\,^1A'$	5.50	2.57	2.09	2.01	1×10^{-3}	1×10^{-5}	2.01
	$1\,^1A''$	1.83	1.89	1.89	1.89	6×10^{-4}	6×10^{-4}	
N2H9	$2\,^1A'$	5.68	2.68	2.18	2.07	9×10^{-4}	1×10^{-8}	2.07
	$1\,^1A''$	1.97	1.98	1.97	1.98	1×10^{-3}	1×10^{-3}	
N2H7	$2\,^1A'$	5.58	2.58	2.09	2.01	2×10^{-2}	4×10^{-5}	2.00
	$1\,^1A''$	1.72	1.82	1.81	1.82	1×10^{-3}	1×10^{-3}	
N2H1	$2\,^1A'$	5.14	2.25	1.80	1.71	2×10^{-2}	3×10^{-5}	1.71
	$1\,^1A''$	1.35	1.47	1.47	1.47	2×10^{-3}	2×10^{-3}	
N3H8	$2\,^1A'$	6.08	3.06	2.57	2.47	8×10^{-4}	3×10^{-6}	2.47
	$1\,^1A''$	2.26	2.31	2.30	2.31	1×10^{-3}	1×10^{-3}	
N3H3	$2\,^1A'$	>5.81	2.97	2.47	2.36	2×10^{-3}	6×10^{-6}	2.36
	$1\,^1A''$	2.18	2.23	2.22	2.23	1×10^{-3}	1×10^{-3}	
N3H7	$2\,^1A'$	5.62	2.71	2.27	2.21	8×10^{-3}	3×10^{-5}	2.21
	$1\,^1A''$	1.92	2.01	2.00	2.01	9×10^{-4}	9×10^{-4}	
N3H2	$2\,^1A'$	5.82	2.79	2.27	2.14	1×10^{-3}	1×10^{-5}	2.14
	$1\,^1A''$	1.86	1.97	1.96	1.97	1×10^{-3}	1×10^{-3}	
N3H4	$2\,^1A'$	5.58	2.67	2.23	2.17	9×10^{-3}	3×10^{-5}	2.17
	$1\,^1A''$	1.90	1.98	1.98	1.98	7×10^{-4}	7×10^{-4}	
N3H5	$2\,^1A'$	5.65	2.68	2.22	2.16	3×10^{-2}	7×10^{-5}	2.16
	$1\,^1A''$	1.78	1.89	1.89	1.89	2×10^{-3}	2×10^{-3}	
N3H6	$2\,^1A'$	5.62	2.64	2.18	2.12	2×10^{-2}	7×10^{-5}	2.12
	$1\,^1A''$	1.70	1.82	1.81	1.82	9×10^{-4}	9×10^{-4}	
N3H9	$2\,^1A'$	5.39	2.41	1.91	1.79	4×10^{-3}	6×10^{-6}	1.79
	$1\,^1A''$	1.50	1.62	1.62	1.62	1×10^{-3}	1×10^{-3}	
N3H1	$2\,^1A'$	5.37	2.45	1.95	1.82	6×10^{-3}	2×10^{-5}	1.82
	$1\,^1A''$	—	1.58	1.58	1.58	2×10^{-4}	2×10^{-4}	

Table 6: Vertical excitation energies (in eV), eBEs (in eV), and oscillator strengths (f) for the acridine derivative anions with dipole moments < 2.0 D.

Molecule	State	pVDZ	apVDZ	apVDZ+4s	apVDZ f	apVDZ+4s f	eBE
N1H5	$2\,^1A_1$	6.22	3.23	2.49	4×10^{-3}	7×10^{-6}	2.49
	$1\,^1B_1$	2.25	2.28	2.28	2×10^{-3}	2×10^{-3}	
N1H4	$2\,^1A'$	5.80	2.77	2.15	2×10^{-2}	2×10^{-5}	2.15
	$1\,^1A''$	1.79	1.87	1.87	5×10^{-4}	5×10^{-4}	
N1H3	$2\,^1A'$	5.69	2.68	2.07	2×10^{-2}	3×10^{-5}	2.07
	$1\,^1A''$	1.61	1.71	1.71	1×10^{-3}	1×10^{-3}	
N2H3	$2\,^1A'$	6.20	2.94	2.35	2×10^{-2}	2×10^{-5}	2.34
	$1\,^1A''$	2.10	2.16	2.16	2×10^{-3}	2×10^{-3}	
N2H4	$2\,^1A'$	6.04	2.96	2.31	3×10^{-2}	9×10^{-6}	2.31
	$1\,^1A''$	2.15	2.18	2.18	9×10^{-4}	9×10^{-4}	
N2H5	$2\,^1A'$	5.64	2.67	2.08	1×10^{-2}	2×10^{-5}	2.08
	$1\,^1A''$	1.89	1.95	1.95	7×10^{-4}	7×10^{-4}	
N2H6	$2\,^1A'$	5.63	2.61	2.00	2×10^{-2}	3×10^{-5}	2.00
	$1\,^1A''$	1.71	1.80	1.80	1×10^{-3}	1×10^{-3}	

Table 7: Vertical excitation energies (in eV), eBEs (in eV), and oscillator strengths (f) for the pyrenidine derivative anions with dipole moments > 2.0 D.

Molecule	State	pVDZ	apVDZ	apVDZ+4s	apVDZ f	apVDZ+4s f	eBE
N1H8	$2\,^1A'$	5.90	2.93	2.44	2×10^{-2}	5×10^{-5}	2.44*
	$1\,^1A''$	2.26	2.33	2.33	2×10^{-3}	1×10^{-7}	
N1H3	$2\,^1A'$	5.95	2.87	2.23	3×10^{-2}	3×10^{-5}	2.23
	$1\,^1A''$	2.13	2.21	2.21	2×10^{-3}	2×10^{-3}	
N1H7	$2\,^1A'$	5.72	2.77	2.22	3×10^{-2}	5×10^{-5}	2.22*
	$1\,^1A''$	1.73	1.86	1.86	3×10^{-7}	3×10^{-7}	
N1H2	$2\,^1A'$	5.61	2.63	2.03	1×10^{-2}	3×10^{-5}	2.03*
	$1\,^1A''$	1.69	1.83	1.83	5×10^{-6}	5×10^{-6}	
N1H9	$2\,^1A'$	5.31	2.38	1.78	7×10^{-3}	2×10^{-5}	1.78*
	$1\,^1A''$	1.61	1.73	1.73	9×10^{-4}	9×10^{-4}	
N1H1	$2\,^1A'$	5.59	2.62	2.05	1×10^{-2}	2×10^{-5}	2.05
	$1\,^1A''$	1.98	2.06	2.06	2×10^{-3}	2×10^{-3}	
N2H2	$2\,^1A'$	5.99	2.97	2.34	2×10^{-2}	3×10^{-5}	2.34*
	$1\,^1A''$	2.08	2.16	2.16	2×10^{-3}	2×10^{-3}	
N2H7	$2\,^1A'$	5.78	2.84	2.36	2×10^{-2}	6×10^{-5}	2.36*
	$1\,^1A''$	2.11	2.19	2.19	2×10^{-3}	2×10^{-3}	
N2H3	$2\,^1A'$	5.75	2.83	2.26	1×10^{-2}	4×10^{-5}	2.25
	$1\,^1A''$	1.96	2.06	2.06	4×10^{-4}	4×10^{-4}	
N2H6	$2\,^1A'$	5.65	2.72	2.18	2×10^{-2}	6×10^{-5}	2.18*[a]
	$1\,^1A''$	3.09	1.79	1.79	4×10^{-6}	4×10^{-6}	
N2H8	$2\,^1A'$	5.68	2.74	2.15	8×10^{-3}	2×10^{-5}	2.15
	$1\,^1A''$	1.89	2.00	2.00	5×10^{-4}	5×10^{-4}	
N2H9	$2\,^1A'$	5.47	2.55	1.97	5×10^{-3}	2×10^{-5}	1.97*
	$1\,^1A''$	1.69	1.79	1.79	6×10^{-4}	6×10^{-4}	
N2H1	$2\,^1A'$	5.56	2.35	1.75	1×10^{-2}	2×10^{-5}	1.75*
	$1\,^1A''$	1.34	1.49	1.49	5×10^{-4}	5×10^{-4}	
N3H4	$2\,^1A'$	5.79	2.82	2.32	2×10^{-2}	1×10^{-3}	2.32*
	$1\,^1A''$	2.28	2.37	2.37	2×10^{-3}	2×10^{-3}	
N3H2	$2\,^1A'$	5.75	2.81	2.25	8×10^{-3}	3×10^{-5}	2.25*
	$1\,^1A''$	2.17	2.29	2.29	8×10^{-4}	8×10^{-4}	
N3H3	$2\,^1A'$	5.73	2.78	2.19	1×10^{-2}	3×10^{-5}	2.19
	$1\,^1A''$	2.10	2.22	2.22	5×10^{-4}	5×10^{-4}	
N3H1	$2\,^1A'$	5.57	2.61	1.99	3×10^{-3}	1×10^{-5}	1.99*
	$1\,^1A''$	1.87	1.98	1.98	1×10^{-3}	1×10^{-3}	

[a] The eBE is computed to be 1.69 eV, but there exist questions about the stability of the Hartree-Fock equations for this computation.

*See Section 3.2.3 for eBE determination for the pyridine derivatives.

Table 8: Vertical excitation energies (in eV), eBEs (in eV), and oscillator strengths (f) for the pyrenidine derivative anions with dipole moments < 2.0 D.

Molecule	State	pVDZ	apVDZ	apVDZ+4s	apVDZ f	apVDZ+4s f	eBE
N1H6	$2\,^1A'$	5.93	2.93	2.41	3×10^{-2}	6×10^{-5}	2.41*
	$1\,^1A''$	2.25	2.33	2.33	3×10^{-3}	3×10^{-3}	
N1H5	$2\,^1A'$	5.75	2.78	2.18	2×10^{-2}	4×10^{-5}	2.18
	$1\,^1A''$	2.01	2.11	2.11	4×10^{-4}	4×10^{-4}	
N1H4	$2\,^1A'$	5.68	2.73	2.15	1×10^{-2}	3×10^{-5}	2.15
	$1\,^1A''$	2.01	2.11	2.11	7×10^{-4}	7×10^{-4}	
N2H5	$2\,^1A'$	5.87	2.89	2.38	3×10^{-2}	7×10^{-5}	2.38*
	$1\,^1A''$	2.14	2.22	2.22	2×10^{-3}	2×10^{-3}	
N2H4	$2\,^1A'$	5.85	2.89	2.30	2×10^{-2}	4×10^{-5}	2.30
	$1\,^1A''$	2.06	2.15	2.15	9×10^{-4}	9×10^{-4}	
N3H5	$2\,^1A_1$	5.87	2.73	2.19	3×10^{-2}	7×10^{-5}	2.19*
	$1\,^1B_1$	2.14	2.03	2.03	0	0	

*See Section 3.2.3 for eBE determination for the pyridine derivatives.